Chromium electroplating and Plasma nitriding to improve the Flow Accelerated Corrosion resistance for the secondary pipe of SMRs

Dong-Ha Kim [a,b], Sunghwan Yeo [a,*], Jun-Hwan Kim [a]
[a]*Next-Generation Fuel Technology Development Division, Korea Atomic Energy Research Institute, Daejeon 34057, Korea*
[*]*Corresponding author: syeo@kiaer.re.kr (Sunghwan Yeo)*

1. Introduction

Nuclear power contributes the growing global demand for energy and becomes an alternative to environmental issues such as carbon neutrality. Small Modular Reactors (SMRs) with a power capacity of 300 MWe or less are advanced nuclear reactors compensate for the supply instability of renewable energy and applicable to various purposes such as industrial energy supply, power sources in remote areas, hydrogen production, and seawater desalination [1]. SMRs obtain high safety and reliability by combining new technologies such as inherent safety system.

As the length of the secondary pipe in SMRs increases when compared to conventional reactors, deterioration phenomena such as flow accelerated corrosion (FAC) and erosion occur rapidly. Moreover, it seems more difficult to diagnose, maintain, and replace the deteriorated pipes due to the use of small diameter piping and the remote areas.

Related technologies include a replacement of new pipes, control of hydrochemical parameters, and surface treatments of pipes [5-8]. In the case of replacing the piping material, the cost is higher than the improvement of hydrochemical parameters and material surface. Low alloy steel with a Cr content of 2.25 wt.% or less has resistance to FAC, but is still vulnerable to erosion. Therefore, in this study, the corrosion and erosion resistance were improved by the electroplating of chromium, which is a classic barrier showing excellent corrosion and wear resistance and applicable to the inner surface of the pipe. Moreover, Cr/ Cr_xN multi-coating layer was formed to further improve the corrosion and wear resistance than the single Chromium layer using plasma nitriding process.

2. Methods and Results

Carbon steel SA-106 was processed into a disk shape with diameter and width of 12 and 2 mm, respectively, and the chemical composition is presented in Table 1. The surface of the specimen were successively polished with 2400 grit SiC abrasive papers and 0.25 μm diamond suspension for uniform deposition.

Table. 1. Carbon steel SA-106 chemical composition

C	Si	Mn	P
0.19	0.25	0.98	0.012
S	Cu	Cr	Ni
0.004	0.02	0.04	0.03
Mo	Ti	Nb	
0.01	0.001	0.008	

2.1 Chromium electroplating

A schematic diagram of a typical electroplating method is shown in Fig. 1. In a general electrochemical method, the target material is the cathode, and the Pb-Sn alloy (9:1 wt.%) is the anode. By applying a constant current, the chromium ions in the electrolyte are induced to attach to the surface by a charge transfer reaction. As a material used for chromium electroplating, a solution obtained by dissolving hexavalent chromic acid in water was used. Chromic acid is dissolved in water to form chromic trioxide as follows:

$CrO_3 + H_2O \rightarrow H_2CrO_4$

These chromic trioxides exist in the form of ions in aqueous solution, and when a potential difference is applied, chromium is deposited on the electrode surface at the cathode as follows [9]:

$CrO_4^{-2} + 8H^+ + 6e^- \rightarrow Cr + 4H_2O$

In the case of the anode, the following reaction is formed:

$2H_2O \rightarrow O_2 + 4H^+ + 4e^-$

A part of the current applied to electroplating is used for the reduction of chromium ions, and a part is consumed for the generation of hydrogen and oxygen on the electrode surface.

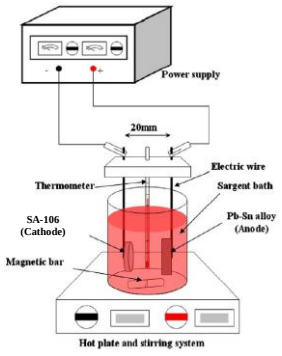

Fig. 1. A schematic diagram of Cr electroplating [9]

In Chromium electroplating, there are several factors that affect the property of plating layer, such as the temperature of plating solution, current density, plating time, and current waveform [10]. Among these, it is

important to develop factors that are easy to manipulate and have a great influence on the characteristics of plating layer and to find the optimum conditions for the plating layer that can effectively prevent FAC.

The plating solution used in this study contains chromium ions, which is a widely used sargent bath (CrO_3 250g/L, H_2SO_4 2.5g/L), and the study was conducted by setting the plating solution temperature, current density as variables. The current waveform was applied by DC.

First, the temperature of the plating bath was increased from 50℃ to 80℃ at 10℃ intervals. And the experimental was performed with a current density and plating time of 88 A/dm^2 and 40 minutes, respectively. As shown in the experimental results in Fig. 2, the thickness of the plating later tends to decrease from 20 μm to 8 μm as the temperature increases, and the size of the precipitated particles increases and the surface becomes rough. And micro-cracks occurred on the surface of the plating layer at 50 ℃. In the case of 60 ℃, it looked like crack-free plating on the surface, but micro-crack were found in the cross-section.

Second, the plating time was carried out from 5 to 80 minutes. As the plating time increases, the Thickness of the plating layer tends to increase for each temperature, but when the plating time elapses 1 hour, the surface becomes rough and micro-cracks occur.

Third, in order to compare the current density, the plating time was carried out for 40 minutes, and the experiment was conducted by applying the current density to 44 ~ 354 A/dm^2 at the temperature range of 60, 65 and 70 ℃. As shown in Table. 2, at a current density of 44 A/dm^2, the thickness decreased to 1/2 at 50 ℃ and 1/4 at 80 ℃. As can be seen in Fig. 3 of the cross-section of the tested specimen by increasing the current density, when the current density was increased over 177 A/dm^2 or more, the thickness of the plating layer decreased rather, micro-crack occurred and the plating later was unevenly generated.

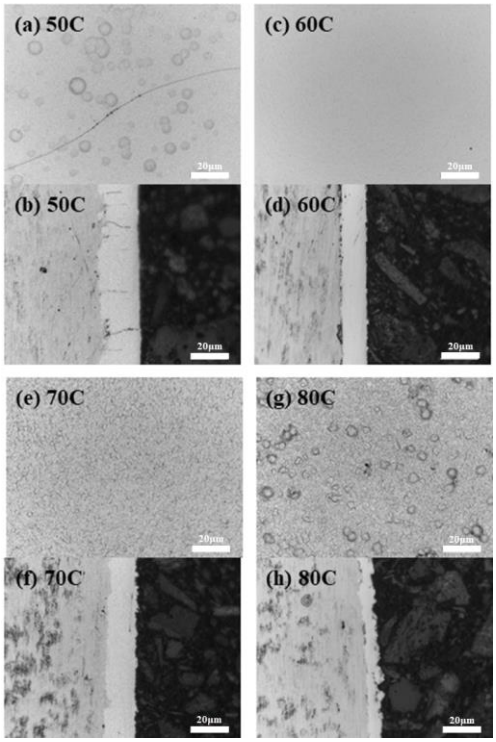

Fig. 2. Optical Micrograph of the surface and cross-section of the electroplating specimen at a temperature in the range of 50 to 80 ℃ for 20 minutes (DC, 88 A/dm^2)

Table2. Cr-coating layer thickness according to electroplating conditions

		300C	600C	1200C	2400C	3600C	4800C
44 A/dm^2	50℃		2	5	10		
	60℃		2	4	8		
	70℃		1	4	8		
	80℃		0	1	2		
88 A/dm^2	50℃	4	6	8	20	12	39
	60℃	4	5	4	13	10	28
	65℃				12		
	70℃	3	5	3	14	14	24
	80℃	0	3	2	8	10	19
177 A/dm^2	60℃				11		
	65℃				11		
	70℃			5	12		
354 A/dm^2	60℃				4~20		
	65℃				2~17		
	70℃			6	2~22		

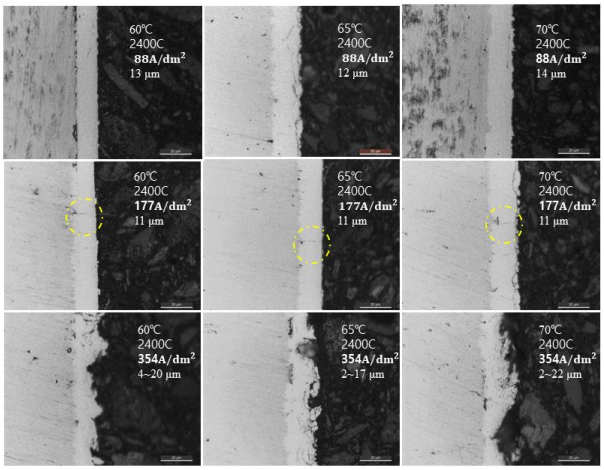

Fig. 3. The cross-section and thickness of the Cr coating layer electroplated for 20 minutes in the temperature range of 60 to 70 ℃ according to the change in current density.

2.2 RF power plasma nitriding

Plasma nitriding was performed on Chromium Coated SA-106 carbon steel specimen using an RF power plasma nitriding system comprising a vacuum chamber, an RF generator, and a power supply. The RF generator utilizes a frequency of 13.56 Hz, a common frequency used to generate plasma ions by ionizing gas molecules such as N_2. The Chromium coated specimen was attached to a specimen holder surrounded by a coiled heating element in a vacuum chamber, and a thermometer was placed near the specimen to check the temperature during test. The internal pressure was maintained at ~10^{-2} Pa, and the N_2-H_2 mixed gas (60:40 in vol.%) was injected while simultaneously venting the gases in the chamber. Since oxidation easily occurs thermodynamically at low partial pressure, H_2 gas was injected to prevent oxidation of the Chromium coating layer. 500W of power was supplied to the RF generator and the nitriding test was conducted at 600 ℃ for 10 to 20 hours.

Fig. 4 shows the cross-section of a nitrided specimen for 10 hours after Chromium electroplating for 20 minutes under direct current and 88 A/dm^2 at 50 ℃ and 70 ℃. In Fig. 4(a), it was confirmed that the nitride was filled in the micro-cracks generated in the electroplating with the nitrided specimen after electroplating at a plating solution temperature of 50 ℃. And since Fig. 4(b) shows the crack-free plating at the plating solution temperature of 70 ℃, the formation of a nitride layer with a thickness of about 1.2 μm on the Chromium plating layer was observed by Energy Dispersive X-ray Spectroscopy (EDS).

Next, a specimen that was Chromium electroplated for 40 minutes was nitrided for 20 hours, as shown in Fig. 5. Figures 5(a) and 5(b) were Cr-coated at 50 and 60 ℃, and the nitride layer did not confirmed. In addition, micro-crack were found after intruding in all temperature range of 50 to 80 ℃, which are crack-free plating conditions. In Fig. 5(c), it was confirmed that micro-crack were recovered due to nitride when nitriding was applied to the specimen plated at 70 ℃, and Fig. 5(d) shows a nitride layer with a thickness of about 1.5 μm was formed on the Chromium plating layer at 80 ℃.

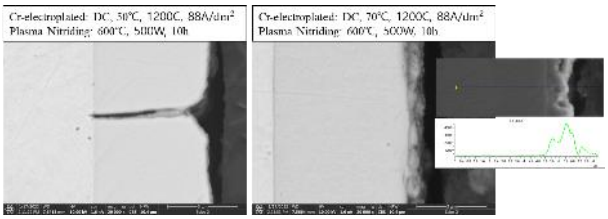

Fig. 4. The cross-sectional optical micrograph of nitrided specimens for 10 hours after Chromium electroplating for 20 minutes under direct current and 88 A/dm2 at (a) 50 ℃ and (b) 70 ℃

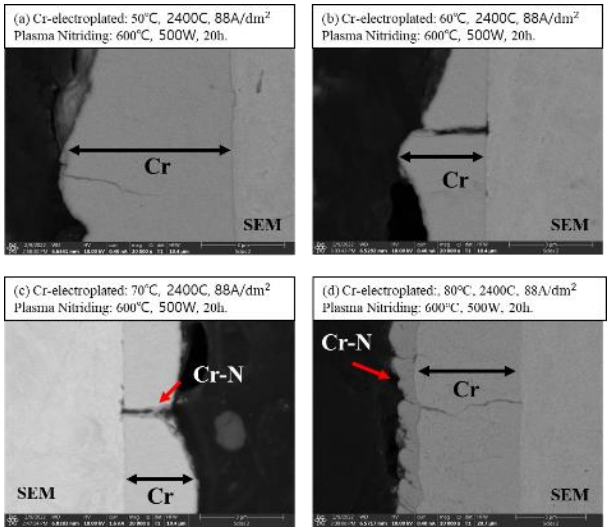

Fig. 5. The SEM micrographs of nitrided specimen for 20 hours under 88A/dm2 with DC.

2.3 Flow Accelerated Corrosion test

The FAC test apparatus is shown in Fig. 6 and constructed using the Rotating Disk Electrode (RDE) test method. The specimen holder was newly designed to test a large number of specimens in the FAC test, and electrochemical test equipment was not installed. Corrosion resistance due to convection of the solution was evaluated by fixing the specimen to the holder and rotating the shaft.

In the FAC test, three types of specimens were used. The first is the as-received SA-106 carbon steel specimen, the second is a specimen plated by applying a current density of 88 A/dm^2 with DC at a plating solution temperature of 50 ℃ and 70 ℃ for 40 minutes, and the third is a nitrided specimen for 20 hours after plating. The amount of the solution is 10 L, and two

type are deionized water and 3.5 wt.% NaCl solution at room temperature.

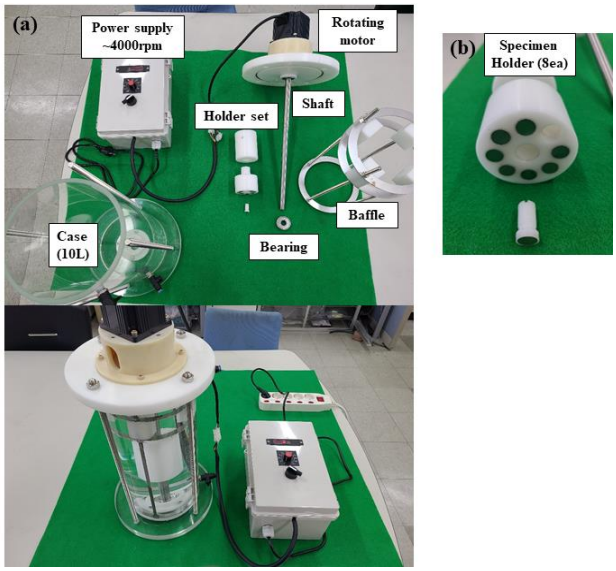

Fig. 6. (a) The Flow Accelerated Corrosion test system including power supply, holder sets, shaft, rotating motor, case, baffle, bearing, and speed controller and (b) specimen holder.

The test results of stationary state and rotating state are shown in Fig. 7 and Fig. 8. When the specimen is placed in a stationary state where the solution do not rotate for 5 hours, the surface of the as-received specimen in deionized water occurred corrosion but weight did not decrease. Then, the test was conducted with 3.5 wt.% NaCl solution. In the NaCl solution, the weight of the as-received specimen decreased by 0.01%, and the weight of the plated specimen at 50 ℃ decreased by 0.0014%. In the plated specimen at 70 ℃, the weight did not decreased, and corrosion did not occurred. When the solution was rotate at 2,000 rpm, the weight of as-received specimen was –0.28 %, which was reduced by about 28 times compared to the stationary state. The weight of the plated specimen at 50 ℃ decreased by 0.007%, while the plated specimen at 70 ℃ did not cause corrosion. It was expected that the nitriding would increase the corrosion resistance, so that the weight loss would be less than that of plating. In the case of the as-received specimen, the weight decreased by 0.18% and the corrosion resistance was improved, but when the FAC test was performed after nitriding the plated specimen, corrosion occurred more easily and the weight decreased significantly. In particular, the plated specimen at 70 ℃ did not corrosion, but after nitriding, the weight loss was 0.16%, which is larger than that of the specimen plated and nitrided at 50 ℃. The first cause of weight loss after nitriding is that during the nitriding process, the specimen holder has a diameter of 11 μm, which is smaller than the diameter of the specimen, so there is a part that is not nitrided. It is expected that corrosion and erosion will occur in this area. The specimen plated and nitrided at 50 ℃ in Fig. 8 had very few traces of corrosion in the nitrided part, but relatively much corrosion occurred in the non-nitriding part. Second, as shown in Fig. 9, crack-free plating was performed at 70 ℃, but cracks occurred in the plating layer during the nitriding process, and it is expected that this will be the path of corrosion.

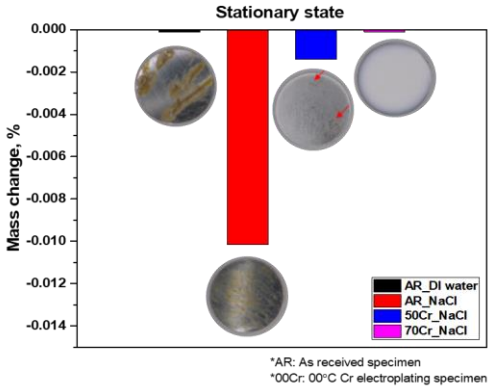

Fig. 7. The weight loss graph and photo for each condition in a stationary state.

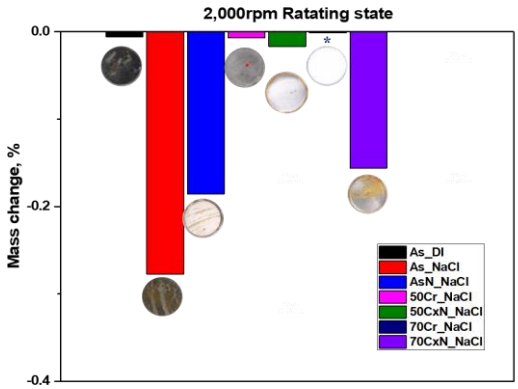

Fig. 8.The weight loss graph and photo for each specimen subjected to FAC test for 5 hours at 2,000 rpm.

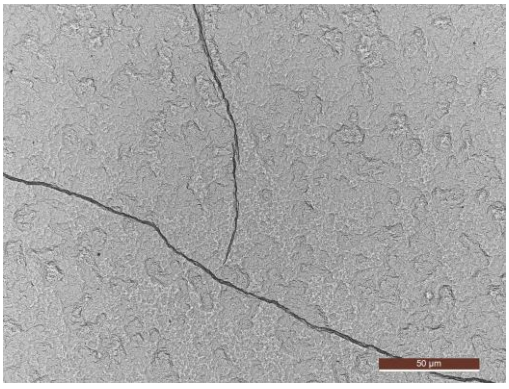

Fig. 9. The optical micrograph of the crack generation on the surface of the nitrided specimen after electroplating at 70 ℃.

3. Conclusions

Chromium electroplating and plasma nitriding are technologies to improve corrosion resistance. As the plating conditions, the thickness of the plating layer is about 20 μm at direct current and a current density of 88 A/dm^2, the cracking temperature is 50 ℃, and the crack-free plating temperature is 70 ℃ with the plating layer thickness of about 13 μm. In the case of 50 ℃ Cr electroplating, after depositing to a thick thickness with fine particles of Chromium, corrosion resistance can be increased by the crack recovery effect of nitriding. In the case of 70 ℃ Cr electroplating, it has excellent corrosion resistance due to crack-free plating. However, as cracks occur during the nitriding process, optimization of the nitriding is require.

In the future research, the nitriding will be optimized to further improve corrosion resistance through chromium plating and nitride compounding, and the mechanism will be elucidated using microstructure analysis. In addition, as a study on the effect of erosion, only half of the specimens are plated, and the FAC test will be conducted.

REFERENCES

[1] HAN, Dengcheng, et al. A Multi-Stochastic SMR Siting Model Applied to the Province of Saskatchewan, Canada: Emphasis on Technological Competition and Policy Impacts. Resources, Conservation and Recycling, Vol. 178, 2022, 106059.
[2] BHOWMIK, Palash Kumar; SCHLEGEL, Joshua Paul, Multicomponent gas mixture parametric CFD study of condensation heat transfer in small modular reactor system safety. Experimental and Computational Multiphase Flow, 2022, 1-14.
[3] OLATEJU, Babatunde; KUMAR, Amit; SECANELL, Marc, A techno-economic assessment of large scale wind-hydrogen production with energy storage in Western Canada. International Journal of Hydrogen Energy, Vol. 41, Issue 21, 2016, Pages 8755-8776.
[4] COOPER, Mark, Small modular reactors and the future of nuclear power in the United States. Energy Research & Social Science, Vol. 3, 2014, Pages 161-177.
[5] Chexal, B., Horowitz, J., & Dooley, B, Flow-accelerated corrosion in power plants, Revision 1 (No. EPRI-TR-106611-R1). Electric Power Research Inst., Palo Alto, CA (United States); Electricite de France (France); Siemens AG Power Generation (Germany), 1998
[6] Lee, Y. B., Lee, J. M., Hur, D. H., Lee, J. H., & Jeon, S. H, Effects of Advanced Amines on Magnetite Deposition of Steam Generator Tubes in Secondary System, Coatings, 2021, 11(5), 514
[7] De Bouvier, O., Bouchacourt, M., & Fruzzetti, K, Redox conditions effect on flow accelerated corrosion: Influence of hydrazine and oxygen, 2002
[8] Sugino, W., Ohira, T., Nagata, N., Abe, A., & Takiguchi, H, Effect of water chemistry improvement on flow accelerated corrosion in light-water nuclear reactor, 2009
[9] Yang, S. W., Ryu, H. J., Kim, J. H., Lee, B. O., & Lee, C. B, FCCI barrier performance of electroplated Cr for metallic fuel", Journal of nuclear materials, 2010, 401(1-3), 98-103
[10] T. H, Webersinn and J. M. Hosdowich, Research Report No. 128, United Chromium, New York, 1932